and also could support inter-laboratory comparisons. However, such standards are not yet available, due to the lack of universal or unequivocally specific markers of EVs, a situation linked to the fact that the content of EVs is probably highly context-dependent. Such tools will therefore only become available with increased knowledge of the core composition and, perhaps, core functions of EVs recovered from diverse sources. Nonetheless, to harmonize research practice in the field of EV research, and to ensure an acceptable level of data comparability, we herein propose that technical and experimental information is provided in significant detail in any published scientific article, and that the characterization includes *a minimal* set of proofs of the EV relationship to the observations reported. We hope that the minimal requirements presented in this editorial therefore will increase awareness of all researchers for potential confounders in their EV-related results, and thus help editors and reviewers of journals other than *J Extracell Vesicles*, less specialized in EVs, to better assess and promote advances in the exceptionally promising field of EV research.

Acknowledgements

We thank J. Kowal, C. Lässer, C. Neri, W. Stoorvogel and M. Tkach for critical comments on this editorial.

Declaration of interest and/or relationship

JL: Co-owner of patents from 2006 to 2012 (approved and pending) for using exosomes as therapeutics. AFH: Co-owner of patent (pending) for using exosomal miRNA as a biomarker; shareholder in D-Gen Ltd. DDV: Inventor of 2 patents on EVs as circulating biomarkers of cancer (pending). YSG: Inventor of patents for using EVs as therapeutics, diagnostics and vaccines; founder of Aeon Medix and own stock in the company; sponsored research agreements with AmorePacific. IK: Co-inventor of a technology for purification of exosomes licensed to Cell Guidance Systems Ltd that uses it for manufacturing Exo-spin™ kits. SS: Co-inventor of a patent (pending) on the use of exosomes as therapeutics in cardiovascular diseases. Sponsored research agreements with Baxter Healthcare and NeoStem. HT: Founder of MiRTeL, and own stock in the company. MHW: Collaborative research agreement with Friesland Campina on bovine milk EVs and with BD Biosciences on high resolution flow cytometry of EVs, and partnership between Technology Foundation STW, Utrecht University and Danone Nutricia research on EV-based biomarker profiling in human breast milk. KWW: Scientific research agreement with AgriSciX, Inc. Other authors declare no significant relationships or conflicts.

Jan Lötvall
Krefting Research Centre
University of Gothenburg, Göteborg, Sweden

Andrew F. Hill
Department of Biochemistry and Molecular Biology
Bio21 Molecular Science and Biotechnology Institute
University of Melbourne, Parkville, Australia

Fred Hochberg
Department of Neurosurgery
University of California at San Diego, San Diego, CA, USA

Edit I. Buzás
Department of Genetics, Cell- and Immunobiology
Semmelweis University, Budapest, Hungary

Dolores Di Vizio
Cedars-Sinai Medical Center, Los Angeles, CA, USA

Christopher Gardiner
Nuffield Department of Obstetrics and Gynaecology
University of Oxford, Oxford, UK

Yong Song Gho
Department of Life Sciences
Pohang University of Science and Technology, Pohang
Republic of Korea

Igor V. Kurochkin
Bioinformatics Institute, Singapore, Singapore

Suresh Mathivanan
Department of Biochemistry
La Trobe University, Melbourne, Australia

Peter Quesenberry
The Warren Alpert Medical School of Brown University
Providence, RI, USA

Susmita Sahoo
Cardiovascular Research Center
Icahn School of Medicine at Mount Sinai, New York, NY, USA

Hidetoshi Tahara
Department of Cellular and Molecular Biology
Hiroshima University Institute of Biomedical & Health Sciences
Hiroshima, Japan

Marca H. Wauben
Department of Biochemistry and Cell Biology
Faculty of Veterinary medicine
Utrecht University, Utrecht, The Netherlands

Kenneth W. Witwer
Department of Molecular and Comparative Pathobiology
Johns Hopkins School of Medicine, Baltimore, MD, USA

Clotilde Théry
INSERM U932, Institut Curie
26 rue d'Ulm, 75005, Paris, France
Correspondence to: clotilde.thery@curie.fr

References

1. Mittelbrunn M, Sanchez-Madrid F. Intercellular communication: diverse structures for exchange of genetic information. Nat Rev Mol Cell Biol. 2012;13:328–35.
2. Boon RA, Vickers KC. Intercellular transport of microRNAs. Arterioscler Thromb Vasc Biol. 2013;33:186–92.
3. van der Grein SG, Nolte-'t Hoen EN. "Small Talk" in the innate immune system via RNA-containing extracellular vesicles. Front Immunol. 2014;5:542.
4. Arroyo JD, Chevillet JR, Kroh EM, Ruf IK, Pritchard CC, Gibson DF, et al. Argonaute2 complexes carry a population

of circulating microRNAs independent of vesicles in human plasma. Proc Natl Acad Sci USA. 2011;108:5003–8.
5. Vickers KC, Palmisano BT, Shoucri BM, Shamburek RD, Remaley AT. MicroRNAs are transported in plasma and delivered to recipient cells by high-density lipoproteins. Nat Cell Biol. 2011;13:423–33.
6. Kalra H, Adda CG, Liem M, Ang CS, Mechler A, Simpson RJ, et al. Comparative proteomics evaluation of plasma exosome isolation techniques and assessment of the stability of exosomes in normal human blood plasma. Proteomics. 2013; 13:3354–64.
7. Van Deun J, Mestdagh P, Sormunen R, Cocquyt V, Vermaelen K, Vandesompele J, et al. The impact of disparate isolation methods for extracellular vesicles on downstream RNA profiling. J Extracell Vesicles. 2014;3: 24858, doi: http://dx.doi.org/10.3402/jev.v3.24858
8. Zonneveld MI, Brisson AR, van Herwijnen MJ, Tan S, van de Lest CH, Redegeld FA, et al. Recovery of extracellular vesicles from human breast milk is influenced by sample collection and vesicle isolation procedures. J Extracell Vesicles. 2014;3: 24215, doi: http://dx.doi.org/10.3402/jev.v3.24215
9. Gould SJ, Raposo G. As we wait: coping with an imperfect nomenclature for extracellular vesicles. J Extracell Vesicles. 2013;2: 20389, doi: http://dx.doi.org/10.3402/jev.v2i0.20389
10. Witwer KW, Buzás EI, Bemis LT, Bora A, Lässer C, Lötvall J, et al. Standardization of sample collection, isolation and analysis methods in extracellular vesicle research. J Extracell Vesicles. 2013;2: 20360, doi: http://dx.doi.org/10.3402/jev.v2i0.20360
11. Hill AF, Pegtel DM, Lambertz U, Leonardi T, O'Driscoll L, Pluchino S, et al. ISEV position paper: extracellular vesicle RNA analysis and bioinformatics. J Extracell Vesicles. 2014;2: 22859, doi: http://dx.doi.org/10.3402/jev.v2i0.22859
12. Kim DK, Lee J, Kim SR, Choi DS, Yoon YJ, Kim JH, et al. EVpedia: a community web portal for extracellular vesicles research. Bioinformatics. 2014, doi: 10.1093/bioinformatics/btu1741.
13. Kalra H, Simpson RJ, Ji H, Aikawa E, Altevogt P, Askenase P, et al. Vesiclepedia: a compendium for extracellular vesicles with continuous community annotation. PLoS Biol. 2012;10: e1001450.
14. Meshorer E, Soreq H. Virtues and woes of AChE alternative splicing in stress-related neuropathologies. Trends Neurosci. 2006;29:216–24.
15. Cvjetkovic A, Lotvall J, Lasser C. The influence of rotor type and centrifugation time on the yield and purity of extracellular vesicles. J Extracell Vesicles. 2014;3: 23111, doi: http://dx.doi.org/10.3402/jev.v3.23111
16. Thery C, Amigorena S, Raposo G, Clayton A. Isolation and characterization of exosomes from cell culture supernatants and biological fluids. Curr Protoc Cell Biol. 2006;Chapter 3:Unit 3 22.
17. Ochieng J, Pratap S, Khatua AK, Sakwe AM. Anchorage-independent growth of breast carcinoma cells is mediated by serum exosomes. Exp Cell Res. 2009;315:1875–88.
18. Shelke GV, Lasser C, Gho YS, Lotvall J. Importance of exosome depletion protocols to eliminate functional and RNA-containing extracellular vesicles from fetal bovine serum. J Extracell Vesicles. 2014;3: 24783, doi: http://dx.doi.org/10.3402/jev.v3.24783
19. Di Vizio D, Morello M, Dudley AC, Schow PW, Adam RM, Morley S, et al. Large oncosomes in human prostate cancer tissues and in the circulation of mice with metastatic disease. Am J Pathol. 2012;181:1573–84.
20. Ginestra A, Monea S, Seghezzi G, Dolo V, Nagase H, Mignatti P, et al. Urokinase plasminogen activator and gelatinases are associated with membrane vesicles shed by human HT1080 fibrosarcoma cells. J Biol Chem. 1997;272:17216–22.
21. Bobrie A, Krumeich S, Reyal F, Recchi C, Moita LF, Seabra MC, et al. Rab27a supports exosome-dependent and -independent mechanisms that modify the tumor microenvironment and can promote tumor progression. Cancer Res. 2012;72:4920–30.

Neurobiology:

Decreased Amyloid-β Pathologies by Intracerebral Loading of Glycosphingolipid-enriched Exosomes in Alzheimer Model Mice

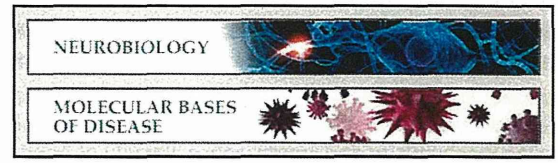

Kohei Yuyama, Hui Sun, Shota Sakai, Susumu Mitsutake, Megumi Okada, Hidetoshi Tahara, Jun-ichi Furukawa, Naoki Fujitani, Yasuro Shinohara and Yasuyuki Igarashi

J. Biol. Chem. 2014, 289:24488-24498.
doi: 10.1074/jbc.M114.577213 originally published online July 18, 2014

THE JOURNAL OF BIOLOGICAL CHEMISTRY VOL. 289, NO. 35, pp. 24488–24498, August 29, 2014

Decreased Amyloid-β Pathologies by Intracerebral Loading of Glycosphingolipid-enriched Exosomes in Alzheimer Model Mice*

Received for publication, April 29, 2014, and in revised form, June 26, 2014 Published, JBC Papers in Press, July 18, 2014, DOI 10.1074/jbc.M114.577213

Kohei Yuyama[‡], Hui Sun[‡], Shota Sakai[‡], Susumu Mitsutake[‡§], Megumi Okada[¶], Hidetoshi Tahara[¶], Jun-ichi Furukawa[‖], Naoki Fujitani[‖], Yasuro Shinohara[‖], and Yasuyuki Igarashi[‡1]

From the [‡]Laboratory of Biomembrane and Biofunctional Chemistry, Graduate School of Advanced Life Science, and Frontier Research Center for Post-Genome Science and Technology, Hokkaido University, Sapporo 001-0021, Japan, [§]Department of Applied Biochemistry and Food Science, Faculty of Agriculture, Saga University, Saga 840-8502, Japan, [¶]Department of Cellular and Molecular Biology, Graduate School of Biomedical Science, Hiroshima University, Hiroshima 734-8553, Japan, and [‖]Laboratory of Medical and Functional Glycomics, Graduate School of Advanced Life Science, and Frontier Research Center for Post-Genome Science and Technology, Hokkaido University, Sapporo 001-0021, Japan

Background: Exosome, a type of extracellular vesicles, can associate with Aβ *in vitro*.
Results: Intracerebrally injected exosomes trapped Aβ on surface glycosphingolipids and transported it into microglia in AD mouse brains, resulting in reductions in Aβ pathology.
Conclusion: Exogenous exosomes act as potent scavengers for Aβ in mouse brains.
Significance: The findings provide a novel therapeutic approach for AD.

Elevated levels of amyloid-β peptide (Aβ) in the human brain are linked to the pathogenesis of Alzheimer disease. Recent *in vitro* studies have demonstrated that extracellular Aβ can bind to exosomes, which are cell-secreted nanovesicles with lipid membranes that are known to transport their cargos intercellularly. Such findings suggest that the exosomes are involved in Aβ metabolism in brain. Here, we found that neuroblastoma-derived exosomes exogenously injected into mouse brains trapped Aβ and with the associated Aβ were internalized into brain-resident phagocyte microglia. Accordingly, continuous intracerebral administration of the exosomes into amyloid-β precursor protein transgenic mice resulted in marked reductions in Aβ levels, amyloid depositions, and Aβ-mediated synaptotoxicity in the hippocampus. In addition, we determined that glycosphingolipids (GSLs), a group of membrane glycolipids, are highly abundant in the exosomes, and the enriched glycans of the GSLs are essential for Aβ binding and assembly on the exosomes both *in vitro* and *in vivo*. Our data demonstrate that intracerebrally administered exosomes can act as potent scavengers for Aβ by carrying it on the exosome surface GSLs and suggest a role of exosomes in Aβ clearance in the central nervous system. Improving Aβ clearance by exosome administration would provide a novel therapeutic intervention for Alzheimer disease.

Alzheimer disease (AD),[2] a common dementia, is pathologically characterized by the presence of amyloid-β peptide (Aβ)-containing senile plaques within the brain. In familial AD, genetic mutations cause increased production of Aβ (1), whereas in far more common sporadic cases, Aβ generation is normal, but its clearance is impaired (2). Elevated levels of Aβ, caused by an imbalance in its metabolism, are linked to synaptic and nerve loss, which likely manifest as progressive cognitive deficits in AD (3).

Exosomes represent a subtype of secreted membrane vesicles (40–100 nm in diameter) of endosomal origin that are released from various types of cells including neurons (4). Exosomes serve to remove and discard unwanted proteins into a drainage system; they are also known to intercellularly shuttle their cargo: a specific set of proteins, RNAs, and lipids (5). Recently, exosomes were reported to associate with a portion of extracellular amyloid-β precursor protein (APP) and its metabolites, including C-terminal fragments (CTFs), amyloid intracellular domain (AICD), and Aβ, in cultures of human wild-type or mutant human APP-expressing neuroblastoma cells (6, 7). In addition, exosomal proteins such as Alix and flottilin-1 were identified around neuritic plaques in AD brains (6). Similarly, our previous study demonstrated that exosomes released from neuroblastoma or primary cortical neurons can bind to synthetic or endogenous Aβ and promote Aβ fibril formation on their surface *in vitro* (8). Furthermore, exosome-bound Aβ is incorporated into microglia for degradation, suggesting that exosomes may act as a mediator for Aβ elimination in brains (8). Here, we demonstrated that long term intracerebral admin-

* This work was supported by Creation of Innovation Centers for Advanced Interdisciplinary Research Areas Program, Ministry of Education, Culture, Sports, Science, and Technology, Japan.
[1] To whom correspondence should be addressed: Laboratory of Biomembrane and Biofunctional Chemistry, Graduate School of Advanced Life Science, and Frontier Research Center for Post-Genome Science and Technology, Hokkaido University, Kita21 Nishi11, Sapporo 00-0021, Japan. Tel.: 81(11)-706-9001; Fax: 81(11)-706-9087; E-mail: yigarash@pharm.hokudai.ac.jp.

[2] The abbreviations used are: AD, Alzheimer disease; Aβ, amyloid-β peptide; APP, amyloid-β precursor protein; GSL, glycosphingolipid; CTF, C-terminal fragment; N2a, Neuro2a; EGCase, endoglycoceramidase; CSF, cerebrospinal fluid; SM, sphingomyelin; Cer, ceramide; GM1, Neu5Acα2-3(Galβ1-3GalNAcβ1-4)Galβ1-4Glcβ1-Cer.

istration of exosomes to the brain of APP transgenic mice resulted in a marked reduction in Aβ levels, amyloid depositions, and Aβ-mediated synaptotoxicity. We also clarified that glycosphingolipids (GSLs) abundant in the exosomes were essential for Aβ binding on the exosome surface.

EXPERIMENTAL PROCEDURES

Cell Cultures—Murine neuroblastoma Neuro2a (N2a) cells were maintained in Dulbecco's modified Eagle's medium (Invitrogen) supplemented with 10% fetal bovine serum. The murine microglial cell line BV-2 was purchased from National Cancer Institute (Istituto Nazionale per la Ricerca sul Cancro, Genova, Italy) and was cultured in RPMI1640 (Invitrogen) supplemented with 10% fetal bovine serum and 2 mM L-glutamine.

Animals—All animal experiments were conducted under a protocol approved by the animal care committees of Hokkaido University. Wild-type C57BL/6 mice were purchased from Japan SLC Inc. (Hamamatsu, Japan). Heterozygotic transgenic mice that express the human APP bearing the Swedish and Indiana (KM670/671NL, V717F) mutations (APP_{swelnd} or J20 strain) were from The Jackson Laboratory (Bar Harbor, ME) and maintained in barrier facilities.

Exosome Isolation—Exosomes were prepared from culture supernatants of N2a cells as described previously (9). Briefly, 1 day before exosome isolation, culture medium was replaced with serum-free medium. The culture supernatants were collected and sequentially centrifuged at 3000 × *g* for 10 min, 4,000 × *g* for 10 min, and 10,000 × *g* for 30 min to remove cells, dead cells, and debris then spun again at 100,000 × *g* for 1 h to obtain exosomes as pellets.

For sucrose gradient analysis, each exosome pellet (100 μg of protein) was loaded onto 10 ml of a sucrose gradient (0.25–2.3 M sucrose in 20 mM HEPES) and centrifuged at 100,000 × *g* for 18 h. After centrifugation, 1-ml fractions were collected, diluted with 20 mM HEPES, and precipitated by centrifugation for 1 h at 100,000 × *g*. The resulting pellets were resuspended in PBS and subjected to Western blot analysis.

Electron Microscopy—Exosomes (100 μg of protein/ml) were resuspended in 50 mM Tris, 150 mM NaCl buffer (pH 7.6) (TBS), and applied to a grid covered with collodion. For Aβ binding experiments exosomes (100 μg of protein/ml) were incubated with $Aβ_{1-42}$ (15 μM) in TBS at 37 °C for 5 h after pretreating with or without EGCase. Exosome mixtures were then applied to the grid. Exosomes were negatively stained with 2% phosphotungstic acid. Transmission images were acquired using an HD-2000 (Hitachi, Tokyo, Japan) or JEM-1400Plus (JEOL Ltd. Tokyo, Japan) transmission electron microscope.

Dynamic Light Scattering—Exosomes (untreated or treated with EGCase) were suspended in TBS at 100 μg of protein/ml. The particle size of the exosomes was measured by dynamic light scattering using a DelsaNano HC (Beckman Coulter).

Injection and Isolation of Biotinylated Exosomes—Exosomes were biotinylated with EZ-link sulfo-NHS Biotin (Pierce) according to the manufacturer's protocol with minor modifications. Briefly, the exosomes were suspended in PBS (150 μg of protein/ml) and incubated with biotin reagent (1 mg/ml) at room temperature for 30 min. The biotinylated exosomes were isolated by ultracentrifugation at 100,000 × *g* for 1 h at 4 °C and resuspended in PBS. For detecting co-precipitated Aβ, 2 μl of the 5 μg/μl biotin-exosome solution was injected into the right hippocampus of APP mouse (4 months old) using stereotaxic coordinates and kept for 3 h. The biotinylated exosomes in the homogenates of the hippocampus were precipitated using streptavidin microbeads according to the protocol in a μMACS streptavidin kit (Miltenyi Biotech, Bergisch Gladbach, German). Co-precipitated Aβ was analyzed with Western blotting or enzyme-linked immunosorbent assay (ELISA) following the solubilization of the exosomes in SDS sample buffer or guanidine buffer, respectively.

SDS-PAGE and Western Blotting—SDS-PAGE and Western blot analysis were performed according to the standard methods of Laemmli. To detect target proteins, we employed as a primary antibody monoclonal antibodies against Alix (BD Bioscience), APP CTFs (Sigma), actin (Sigma), Aβ (6E10, Signet, Dedham, MA), or neprilysin (Santa Cruz Biotechnology) or rabbit polyclonal antibodies against flottilin-1, endothelin converting enzyme-1 (ECE-1), (Santa Cruz Biotechnology), or insulin degrading enzyme (IDE, Abcam) and as a secondary antibody an anti-mouse IgG-HRP antibody(GE Healthcare), or anti-rabbit IgG-HRP antibody (GE Healthcare). To detect the ganglioside GM1, we used horseradish peroxidase-conjugated cholera toxin B subunit from Sigma. Bands were visualized using a combination of an ECL Plus kit (GE Healthcare) and an LAS4000 imaging system (Fuji Film, Tokyo).

Fluorescence Labeling for the Exosomes—Exosomes were stained with the red fluorescence dye PKH26 (Sigma) as described previously (8). Briefly, the exosomes were resuspended in diluent C (Sigma) and incubated with PKH26 at room temperature for 5 min. The reaction was stopped by the addition of 1% bovine serum albumin. The PKH26-labeled exosomes were precipitated again by ultracentrifugation at 100,000 × *g* at 4 °C for 1 h.

Exosome Isolation from Murine Cerebrospinal Fluid (CSF)—CSF was collected from the cisterna magna of 2-month-old C57BL/6 mice as previously described (10). Exosomes were isolated from the CSF using a method similar to that described above for isolation from culture medium.

Analysis of Exosomal Particle Number—A qNano System (Izon Science, Ltd) was employed to analyze the particle densities of N2a- and mouse CSF-derived exosomes resuspended in PBS.

Exosome Administration in Mouse Brains—Mice were continuously treated with exosome solution (2 mg protein/ml) or vehicle (PBS) by Alzet minipump (model 1002) at 0.25 μl/h for 14 days. Mice were placed in a stereotactic instrument (NARISHIGE, Tokyo, Japan), and stainless steel cannulas of Alzet Brain Infusion Kit3 were implanted into the right lateral ventricle (mediolateral, −0.8 mm; dorsoventral −3.0 mm) or hippocampus (anteroposterior, −2.0 mm; mediolateral, −1.3 mm; dorsoventral −2.2 mm). After a 14-day infusion, mice were then transcardially perfused with cold heparin/PBS. The right hemibrain was fixed with 4% paraformaldehyde, PBS at 4 °C for 48 h for use in immunohistochemistry, and the left hemibrain was rapidly frozen with liquid nitrogen and stored at −80 °C for later analysis.

For single injection studies, PKH-labeled exosomes or a conjugate of PKH-exosomes with fluorescent Aβ (4 μg of exosome protein in 2 μl PBS) were injected into the right hippocampus or the lateral ventricle of non-transgenic mice using stereotaxic coordinates as described above. To obtain the conjugates of the exosomes with Aβ, PKH-exosomes (100 μg/ml) were incubated with $Aβ_{1-40}$ in TBS at 37 °C for 24 h then centrifuged at 100,000 × *g* for 1 h to remove free Aβ. At 3 or 24 h post injection, the mouse brains were prepared as described above for immunohistochemistry.

Immunohistochemistry—The tissue sections were cut with a cryostat (Leica CM3050S) and post-fixed with 4% paraformaldehyde, PBS. After blocking with 5% bovine serum albumin (BSA), 16-μm-thick sections were immunostained with monoclonal antibodies against Iba1 (Wako), βIII tublin (Promega), or glial fibrillary acidic protein (SHIMA laboratory) followed by visualization with AlexaFluor488-conjugated anti-IgG. Serial 30-μm thickness of brain sections were immunostained with monoclonal antibody against Aβ (4G8, Covance) after a brief formic acid treatment, and the signals were visualized using ABC elite kit (Vector Laboratories). Confocal images were obtained using an Olympus Fluoview FV10i microscope. The Aβ plaques were estimated as the percentage of the immunopositive area (positive pixel) to the examined area (total pixel) using ImageJ software.

Aβ ELISA—Aβ levels were determined using a sandwich ELISA. The kits for $Aβ_{1-40}$ and $Aβ_{1-42}$ were obtained from Wako (Osaka, Japan), and that for $Aβ_{1-38}$ was from IBL (Gunma, Japan). Mouse hippocampus or exosomes were homogenized in 4 M guanidine-HCl buffer (pH 8.0) with an ultrasonic homogenizer (TAITEC, Saitama, Japan). After incubation at room temperature for 3 h, the homogenates were further diluted with 0.1% BSA, PBS and centrifuged at 16,000 × *g* for 20 min. The resulting supernatants were then applied to the ELISA. All samples were measured in duplicate.

Evaluation of Synaptic Densities—Synaptophysin-immunoreactive synaptic densities were quantified according to the methods of Mucke *et al.* (11) with minor modifications. The right hemisphere of each APP mouse brain was sagittally cut into 16-μm-thick sections using a freezing microtome. The serial sections were incubated with a monoclonal antibody against synaptophysin (D35E4, Cell Signaling) followed by incubation with AlexaFluor488-bound anti-IgG. Immunofluorescent signals were visualized using an Olympus Fluoview FV10i microscope. The linear range of the synaptophysin-positive fluorescence intensities in nontransgenic control sections was determined, and the same setting was used to analyze all of the following images. For each mouse 9 confocal images were captured in three sections per the right hemisphere of the brain, and each image covered an area 5500 $μm^2$ in the molecular layer of the dentate gyrus. The synaptophysin-immunoreactive synaptic densities were estimated as a percentage of the immunostained area (positive pixel) to the selected image area (total pixel) using ImageJ software.

Thioflavin-S Staining—Brain sections (30 μm thick) were oxidized with 0.25% potassium permanganate for 20 min followed by 3 min of bleaching in 2% potassium metabisulfite and 1% oxalic acid. Sections were stained with 0.015% thioflavin-S in 50% ethanol in the dark for 10 min. After developing in two changes of 50% ethanol for 4 min each, images were captured with Olympus Fluoview FV10i microscope, and thioflavin-S-positive plaques were counted in three sections per mouse hippocampus.

Measurement of GSLs—The extraction of GSLs from the culture cells and the exosomes, the enzymatic digestion of GSL-glycans with EGCase I and II (Takara Bio, Shiga, Japan), and the purification of glycans using glycoblotting were performed as described previously (12). Purified GSL-glycans were analyzed by MALDI-TOF MS using an Ultraflex II TOF/TOF mass spectrometer equipped with a reflector, which was controlled by the FlexControl 3.0 software package (Bruker Daltonics, Bremen, Germany). All spectra were obtained as positive ions and were annotated using the FlexAnalysis 3.0 software package (Bruker Daltonics). The glycan structures were then identified by online database SphinGOMAP.

Quantification of Cholesterol, Sphingomyelin (SM), Ceramide (Cer), and Phosphatidylcholine—Total lipids were extracted from the exosomes or N2a cells by adding chloroform/methanol (1:2, v/v). Levels of sphingomyelin SM and Cer were determined by electron ionization-mass spectrometry (TripleTOF™ 5600) coupling with PeakView software (AB SCIEX, Framingham, MA). Cer (C16:0, d18:1) and SM (C16:0, d18:1) were purchased from Avanti Polar Lipids (Alabaster, AL) and were used as standards. The amounts of and cholesterol were measured by a phosphatidylcholine assay kit (BioVision, Milpitas, CA) and cholesterol E-test kit (Wako), respectively.

Proinflammatory Cytokine ELISA—The levels of proinflammatory cytokines, including tumor necrosis factor-α (TNF-α), interleukin-6 (IL-6), IL-1β, and interferon (IFN-γ), were determined by ELISA (Multi-Analyte ELISArray, Qiagen) according to the manufacturer's instructions. Briefly, each APP mouse hippocampus was homogenized in 4 M guanidine-HCl buffer (pH 8.0) using an ultrasonic homogenizer (TAITEC). After an incubation at room temperature for 3 h, the homogenates were further diluted in 0.1% BSA, PBS and centrifuged at 16,000 × *g* at 4 °C for 20 min. The resulting supernatants were applied to the ELISA. All samples were handled in duplicate.

EGCase and Sialidase Treatment—Exosomes (1 mg of protein/ml) were incubated with 0.5 units/ml EGCase II (Takara Bio Inc., Shiga, Japan) at 37 °C for 15 h in PBS containing 20 mM HEPES (pH 7.4) or 1 unit/ml of sialidase from *Clostridium perfringens* (Sigma) at 37 °C for 16 h in 50 mM acetate buffer (pH 5.5). Each mixture was centrifuged at 100,000 × *g* for 1 h. The resultant precipitates were resuspended in TBS or Hepes-buffered saline and used for further examination.

Seed-free Aβ Preparation—Seed-free Aβ solutions were prepared essentially according to a published report (13).

Aβ Binding Assay—PKH26-labeled exosomes (untreated or treated with EGCase) were plated on chamber slideglass (Thermo Fisher Scientific, Waltham, MA) by staying in PBS for 1 h at room temperature. Fluorescence-labeled $Aβ_{1-42}$ (1 μM) was then added into the chamber of cultured N2a cells or the labeled exosomes and co-incubated in serum-free medium at 37 °C for 5 h. After a wash with PBS to remove free Aβ, fluores-

cent images were captured using Olympus Fluoview FV10i microscope.

Binding Analysis by Surface Plasmon Resonance—The binding studies of N2a-derived exosomes (untreated or pretreated with EGCase) with immobilized Aβ peptide ($Aβ_{1-40}$, $Aβ_{1-42}$, $Aβ_{1-38}$, or $Aβ_{42-1}$) were performed using BIACORE T200 instrument (GE Healthcare). Briefly, seed-free Aβ was independently immobilized onto a carboxymethylated (CM) dextran-coated gold surface (CM5 sensor chip) by amine coupling. The amount (resonance units.) of immobilized $Aβ_{1-40}$, $Aβ_{1-42}$, $Aβ_{1-38}$, or $Aβ_{42-1}$ was 1143.0, 1266.7, 1316.3, or 948.0, respectively. Then the exosomes were suspended in Hepes-buffered saline (10 mM HEPES, 150 mM NaCl (pH 7.4)) and injected over the surface at 25 °C for 1 min at a flow rate of 30 μl/min. The resultant responses were subtracted from a blank that was immobilized with BSA or prepared by ethanolamine deactivation. Finally, the exosomes were regenerated from the Aβ-immobilized surface by injecting 5 M guanidine-HCl, 10 mM Tris-HCl (pH 8.0).

Thioflavin-T Assay—Seed-free $Aβ_{1-42}$ solutions (15 μM) were incubated at 37 °C for various times with the exosomes (100 μg of protein of exosomes in 100 μl of TBS) that had been untreated or treated with EGCase. Fluorescence intensities of Thioflavin-T (Sigma) were determined as described before (8) using an Appliskan spectrofluorophotometer (Thermo Fisher Scientific).

Exosome Uptake Assay—Uptake of PKH26-labeled exosomes into microglial BV-2 cells were measured as described previously (8). Briefly, fluorescent exosomes were administered to BV-2 cells and incubated for various times in serum-free conditions. After a wash, the cells were then fixed, and confocal images were acquired using an Olympus Fluoview FV10i microscope. The fluorescence intensity of each sample was analyzed with ImageJ software.

RESULTS

Exogenously Injected Exosomes Trap Aβ and Are Incorporated into Microglia in Mouse Brains—To explore the hypothesis that providing exogenous exosomes *in vivo* would enhance Aβ clearance by facilitating engulfment of exosome-bound Aβ by microglia, we loaded isolated exosomes into mouse brains and evaluated the effect on the balance of Aβ metabolism. Exosomes were collected from culture supernatants of mouse neuroblastoma N2a cells using sequential ultracentrifugation; the exosomes typically consisted of membrane vesicles of 70–120 nm in diameter (Fig. 1, *A* and *B*) as previously described (14). The presence of exosomes was confirmed by detecting the exosomal markers Alix and flotillin-1 as well as the membrane glycolipid GM1 ganglioside in sucrose density gradient fractions corresponding to a density of 1.12 and 1.16 g/ml (Fig. 1*C*). Aβ was not identified in N2a cells and the exosomes used in this study (Fig. 1*C*). Exosomes isolated from N2a cells were biotinylated and injected into the hippocampus of APP_{SweInd} transgenic (APP) mice. Hippocampal Aβ was detectable in streptavidin-precipitated exosomes together with the marker Alix 3 h after the injection (Fig. 1*D*). Accompanied by Aβ, the intrahippocampal-injected exosomes co-localized with the microglial marker Iba1 (Fig. 1*E*), agreeing with our previous *in vitro* study

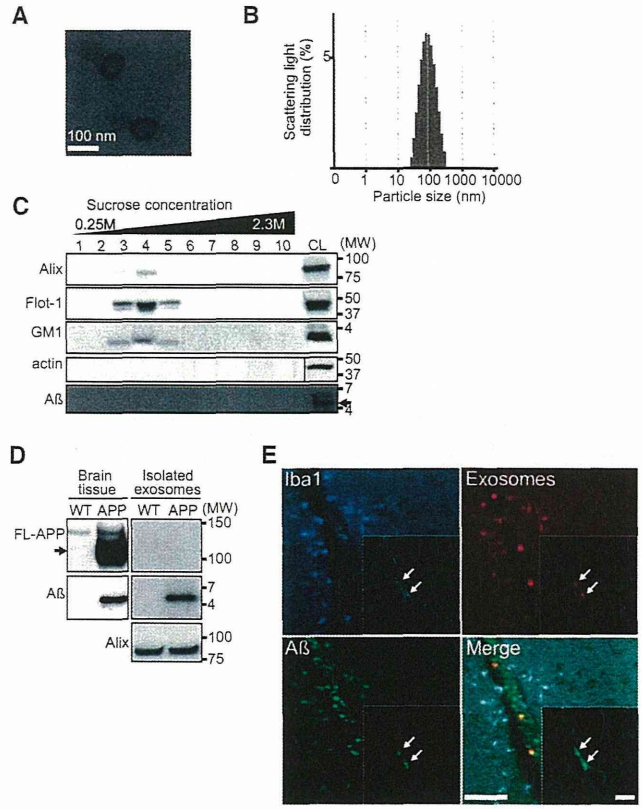

FIGURE 1. **Exogenously injected exosomes trap Aβ and are internalized into microglia in mouse brains.** Exosomes were isolated from culture supernatant of N2a cells by sequential centrifugation, eventually to 100,000 × *g* pellets. *A*, an electron microscopic image of phosphotungstic acid-stained exosomes. *B*, exosomes were measured by dynamic light scattering. *C*, exosomes were density-fractionated by sucrose gradient, and the fractions were analyzed by Western blotting to detect the exosome markers Alix, flotillin-1 (*Flot-1*), and ganglioside GM1 (*GM1*) as well as actin and Aβ. *CL*, cell lysates. *D*, biotinylated exosomes stereotaxically injected into the hippocampus of 4-month-old non-transgenic or APP mice were isolated using biotin binding affinity beads, then analyzed by Western blotting to detect co-precipitated full-length (*FL*)-APP, Aβ, and Alix. *E*, conjugates of fluorescence-labeled Aβ (*green*) and exosomes (*red*) were administered into the hippocampus of non-transgenic mice. The hippocampal images were captured 3 h after the injection, following antibody staining for the microglial marker Iba1 (*blue*). *Scale bar*, 50 μm and 10 μm (*inset*).

(8). These results demonstrate that in mouse brains exogenous exosomes bind Aβ and are then incorporated into microglia together with the bound Aβ for degradation.

Continuous Exosome Administration Ameliorates Aβ Pathology and Synaptic Dysfunction in APP Mouse Brains—we next continuously administered exosomes into the lateral ventricles of 4-month-old APP mice for 14 days using osmotic minipumps. The exosome solution (2 mg of protein/ml) contained 2.67×10^{12} particles/ml, which is ~35 times higher than the concentration of the exosomes in mouse CSF (7.51×10^{10} particles/ml). The intraventricularly injected exosomes have been reported to penetrate into brain parenchyma (15). After 2 weeks, there was an approximate 50% reduction in total $Aβ_{1-40}$ and $Aβ_{1-42}$ levels and 35% reduction in $Aβ_{1-38}$ levels in the hippocampus of the exosome-treated APP mice compared with those infused with vehicle (Fig. 2*A*). A similar decline in Aβ levels was confirmed by direct administration of the exosomes into mouse hippocampus, with ~50% less observed in the ipsi-

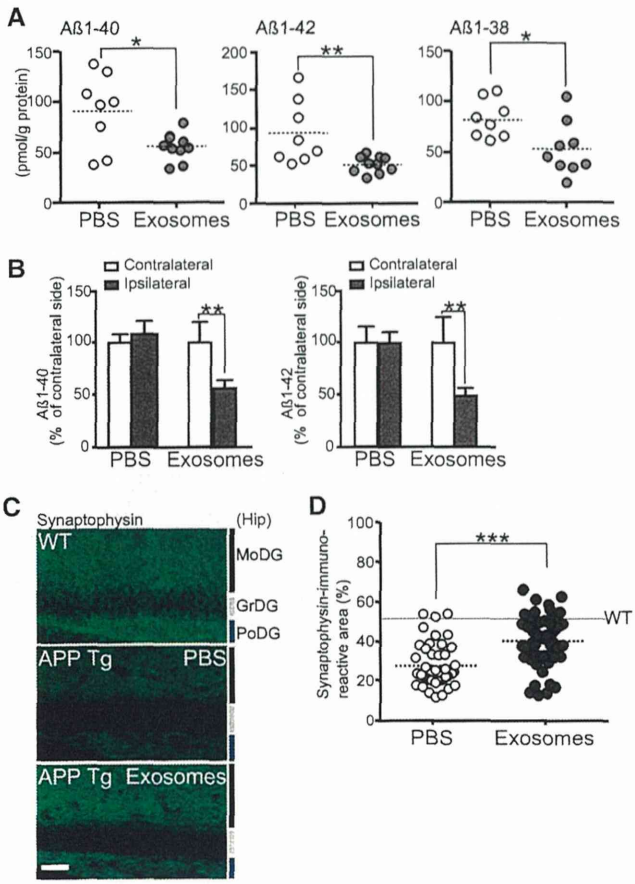

FIGURE 2. **Intracerebral administration of N2a-exosomes induces Aβ clearance.** Exosomes (12 μg of protein/PBS/day) or vehicles were continuously infused into lateral ventricle (*A*, *C*, and *D*) or right hippocampus (*B*) of APP mice (4 months) for 14 days. *A*, after the infusion, hippocampal levels of Aβ were measured by ELISA ($n \geq 5$ animals per group; mean ± S.D.; *, $p < 0.05$; **, $p < 0.01$; Student's *t* test). *B*, hippocampal Aβ levels in ipsilateral and contralateral side were measured by ELISA. Values are represented as the percentages of the Aβ levels in the contralateral side (PBS, $n = 3$; exosome, $n = 4$; mean ± S.D.; **, $p < 0.01$; Student's *t* test). *C*, representative hippocampal sections of exosome- or vehicle-infused APP mice or age-matched non-transgenic controls stained with antibody against synaptophysin. *MoDG*, molecular dentate gyrus (*DG*); *GrDG*, granular DG; *PoDG*, polymorph DG. *Scale bar*, 100 μm. *D*, densities of synaptophysin-positive presynaptic terminals in the hippocampal sections in *C* were quantified (5 sections/mouse, 5 mice per group). Data presented are the mean ± S.D. ***, $p < 0.001$.

lateral injection side than the contralateral (Fig. 2*B*). APP mice given vehicle treatment exhibited ~50% decreased densities in synaptophysin immunoreactivities in the hippocampus as compared with wild-type mice (Fig. 2, *C* and *D*), agreeing with previous reports (11). After a 14-day infusion of the exosomes, the synaptophysin immunoreactivities were markedly increased in the APP mouse hippocampus (85 and 50% of those observed in WT mice after exosome and PBS treatment, respectively; Fig. 2*D*). Thus, the exosomes mediated significant recovery from synaptic impairment in the APP mice. Taken together, these findings validated that *in vivo*, exogenously added exosomes induce reductions in Aβ levels and Aβ-associated synaptotoxicity.

To assess the effect of exogenous exosomes on brain amyloid deposition, we continuously administered the exosomes into the hippocampus of 13-month-old APP mice for 14 days. We found that the exosomes markedly decreased the Aβ immunoreactive burden (65% reduction; Fig. 3, *A* and *B*) and number of thioflavin-S-positive plaques (38%; Fig. 3*C*) in the treated hippocampus compared with the untreated side. Supporting these histological results, tissue levels of $A\beta_{1-40}$ and $A\beta_{1-42}$ were also significantly decreased after exosome infusion, as determined by ELISA (Fig. 3*D*). We also performed exosome infusion into the lateral ventricles of 13-month-old APP mice for 14 days and found significant reductions in $A\beta_{1-40}$ and $A\beta_{1-42}$ levels in the mouse hippocampus (Fig. 3*E*). These findings demonstrate the evident efficacy of long term treatment with exogenous exosomes in Aβ deposition, even deposition of the fibrillar species of Aβ aggregates, in APP mice.

To exclude the possibility that the changes observed *in vivo* are due to effects of exosomes on Aβ generation and enzymatic degradation, we examined the expression levels of APP and its cleaved fragments, including CTF-α and CTF-β, in the hippocampus. No obvious differences in the expression levels were apparent between the exosome- and PBS-treated APP mice (Fig. 4*A*). In addition, the expression levels of well known proteases for Aβ peptides, including insulin-degrading enzyme, neprilysin, and angiotensin-converting enzyme, were investigated, but there were no variations even after exosome infusion (Fig. 4*A*). Although the exogenous exosomes were taken up by the microglia, there was no obvious activation in releasing the proinflammatory cytokines like TNFα, IL-6, IL-1β, or IFN-γ in the exosome-treated mouse hippocampus (Fig. 4*B*). The above findings indicate that the exosomes reduce Aβ levels by promoting an alternative pathway for Aβ clearance, *i.e.* exosome-associated Aβ uptake by microglia, without any stimulation in APP processing, Aβ degradation, or microglial inflammatory reactions.

Exosomal GSL-glycans Are Critical for Their Association with Aβ in Vitro and in Vivo—The above experiments clearly indicate that the exogenous exosomes associated with the Aβ in the mouse brains, although how they interact with each other remained to be determined. Increasing evidence with synthetic liposomes or membranes has demonstrated that gangliosides (sialic acid-containing GSLs) clustering on the membrane surface bind to Aβ and that this Aβ-GSL complex then acts as a template for catalyzing the reaction of Aβ fibril formation (16, 17). *In vivo*, the monosialoganglioside GM1 was found to associate with Aβ in human brains that exhibit AD pathology (18, 19). GSLs are reported to exist in exosomes (6), but details regarding which species of GSLs have not yet been described. We summarized the profiles of GSL-derived glycans from the exosomes and the cells from which the exosomes derived by quantitative GSL-glycomics (Table 1). The total amount of GSLs was much higher in exosomes than in the parent cells (~2300%, Fig. 5*A*). In either, the vast majority of GSLs were GM2 (>84%), with distinct minor compositions (Table 1). Except for GM2, the levels of sialylated GSLs were much higher in the exosomes (Fig. 5*B*). To investigate whether the GSLs abundant in the exosomes might affect Aβ binding and fibril formation, we deglycosylated exosomal GSLs using EGCase, which specifically cleaves the linkage between the oligosaccharide and glucosylceramide in GSLs (20). The particle size of the exosomes was stable up to 5 h after EGCase digestion, although

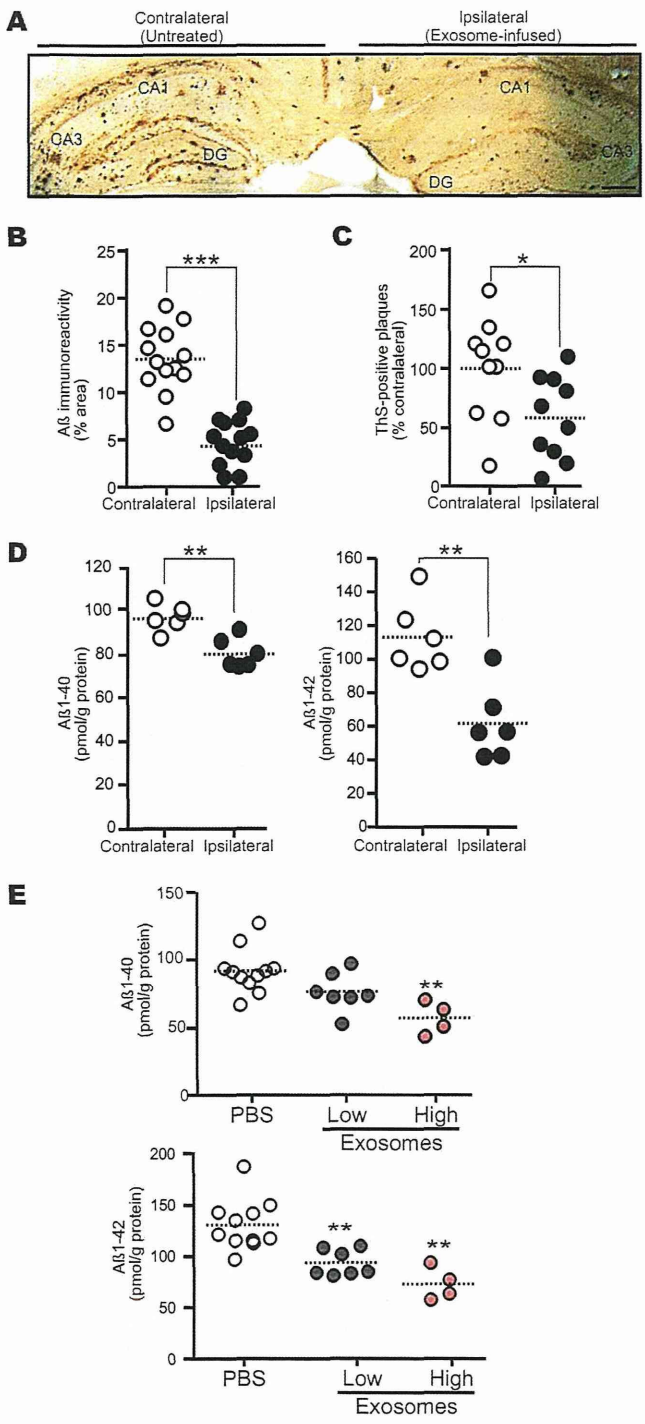

FIGURE 3. **Intracerebral administration of N2a-exosomes reduces Aβ deposition.** Exosomes (12 μg of protein/PBS/day) were continuously infused into the hippocampus (*A–D*) or lateral ventricle (*E*) of 13-month-old APP mouse for 14 days. *A*, representative image of APP mouse hippocampal section stained with antibody against Aβ (4G8). *DG*, dentate gyrus. *Scale bar*, 200 μm. *B*, Aβ-immunopositive areas in each hippocampal region were quantified ($n = 4$ animals, 3 or 4 sections per mouse brain; ***, $p < 0.001$). *C*, the number of thioflavin-S (*ThS*)-positive plaques in each hippocampus was determined ($n = 4$ animals, 2 or 3 sections per a brain; *, $p < 0.05$). *D*, the levels of hippocampal $A\beta_{1-40}$ and $A\beta_{1-42}$ were measured by ELISA ($n = 3$ animals, assayed in duplicate; **, $p < 0.01$). *E*, exosomes (low, 12 μg of protein/PBS/day; high, 24 μg of protein/PBS/day) were infused. Hippocampal Aβs were measured by ELISA ($n \geq 4$ animals per group; **, $p < 0.01$ compared with PBS).

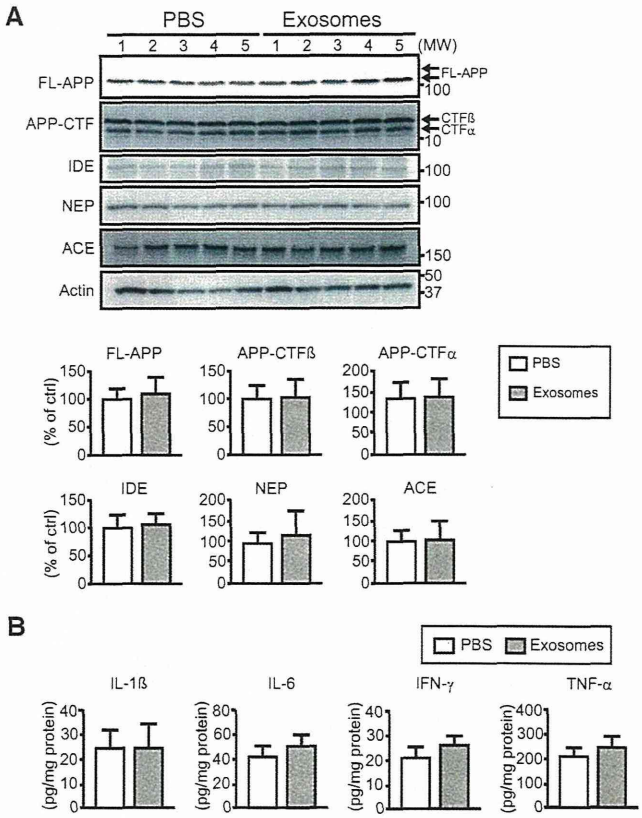

FIGURE 4. **Exogenous exosomes do not stimulate APP processing, expressions of Aβ-degrading enzymes, or inflammatory response.** Exosomes or PBS were continuously infused into the lateral ventricles of APP mice (4 months old) for 14 days (*A* and *B*). $n \geq 5$ animals per group. *A*, full-length (*FL*)-APP, APP-CTFs, and the Aβ-degrading enzymes insulin-degrading enzyme (*IDE*), neprilysin (*NEP*), and angiotensin-converting enzyme (*ACE*) were detected in the hippocampus by Western blotting, and the intensity for each band was quantified. Data presented are the mean ± S.D. *B*, expression levels of proinflammatory cytokines (IL-1β, IL-6, IFN-γ, and TNF-α) in the hippocampus were measured by ELISA. Data are the mean ± S.D.

larger aggregates commonly formed during the 24-h incubation (Fig. 5*C*). Within the 5-h period, the EGCase-treated exosomes associated very little with the Aβ, as compared with intact exosomes, which overtly colocalized with the Aβ (Fig. 5*D*).

We performed surface plasmon resonance studies to evaluate the specificity of the interaction between N2a-derived exosomes and individual Aβs. As shown in Fig. 5*E*, when the exosomes were injected onto the immobilized $A\beta_{1-42}$ and $A\beta_{42-1}$, a peptide with reverse sequence of $A\beta_{1-42}$, only the former gave a significant increase in resonance signal, demonstrating the specific nature of the interaction. Specific interactions of the exosomes were observed not only with immobilized $A\beta_{1-42}$ but also with $A\beta_{1-40}$ and $A\beta_{1-38}$, and we found that the interactions were almost completely diminished when the exosomes were pretreated with EGCase (Fig. 5*F*). These results suggest that Aβs directly binds to the exosomes through the GSL glycans, particularly those sialic acid moieties on their surface. Pretreatment with EGCase also inhibited exosome-dependent amyloid fibril formation in incubation mixtures of exosomes and $A\beta_{1-42}$, as assessed by thioflavin-T assay and electron microscopic observation (Fig. 6, *A* and *B*). Cleavage of sialic

TABLE 1
Summary of GSL-glycans found in exosomes and their parental N2a cells
Gg, ganglio-series; Gb, globo-series; Lc, lacto-series.

No.	Composition	Class	Name	Absolute quantity (pmol/mg protein)		Relative quantity (%)	
				Cells	Exosomes	Cells	Exosomes
1	(Hex)2(Neu5Ac)1	Gg	GM3	9.142	210.686	1.111	1.108
2	(Hex)2(HexNAc)1(Neu5Ac)1	Gg	GM2	693.815	16095.765	84.284	84.667
3	(Hex)2(HexNAc)1(Neu5Gc)1	Gg	GM2(Gc)	6.866	328.257	0.834	1.727
4	(Hex)2(Neu5Ac)2	Gg	GD3	0.000	5.067	0.000	0.027
5	(Hex)3(HexNAc)1(Neu5Ac)1	Gg	GM1	1.359	102.665	0.165	0.540
6	(Hex)3(HexNAc)1(Neu5Gc)1	Gg	GM1(Gc)	0.000	2.011	0.000	0.011
7	(Hex)3(HexNAc)1(Neu5Ac)2	Gg	GD1	0.833	489.823	0.101	2.577
8	(Hex)3	Gb	Gb3	0.000	883.100	0.000	4.645
9	(Hex)3(HexNAc)1	Gb	Gb4	1.884	4.378	0.229	0.023
10	(Hex)4(HexNAc)1-SSEA3	Gb	Gb5	3.684	0.000	0.448	0.000
11	(Hex)3(HexNAc)1	(n)Lc	(n)Lc4	12.654	198.461	1.537	1.044
12	(Hex)4(HexNAc)1	(n)Lc	Gal-(n)Lc4	3.684	24.117	0.448	0.127
13	(Hex)3(HexNAc)1(Fuc)2	(n)Lc	diFuc-(n)Lc4	0.000	9.987	0.000	0.053
14	(Hex)3(HexNAc)2(Fuc)1	(n)Lc	Fuc-(n)Lc5	0.922	7.729	0.112	0.041
15	(Hex)4(HexNAc)2	(n)Lc	nLc6	0.000	3.347	0.000	0.018
16	(Hex)5(HexNAc)2	(n)Lc		0.204	1.875	0.025	0.010
17	(Hex)4(HexNAc)2(Fuc)1(NeuAc)2	(n)Lc		0.337	0.000	0.041	0.000
18	(Hex)2(HexNAc)1	-	Lc3/aGM2	87.803	643.481	10.666	3.385
			total	823.189	19010.751	100.000	100.000

acids with sialidase resulted in similar reductions in fibril formation (Fig. 6*C*). Steric blocking of GM1 or GM2 ganglioside by cholera toxin subunit B or anti-GM2 antibody, respectively, also partially but significantly suppressed amyloid formation (Fig. 6*C*). In contrast to intact exosomes, the EGCase-treated exosomes nearly failed to coprecipitate with Aβ when injected into the hippocampus of APP mice (Fig. 6*D*). Our data verify that cleavage of GSL glycans from exosomes can sufficiently prevent the association of exosomes with Aβ. This suggests that there may be multiple species of GSLs, especially sialylated forms, on exosomal membranes that organize into unique sites of high potency able to induce Aβ binding and assembly.

In addition to gangliosides, cholesterol and SM are also known to promote Aβ assembly via the lateral packing of gangliosides on membranes (21, 22). We found that both cholesterol and SM were highly abundant in exosomes compared with their parent cells (Fig. 7), suggesting that high densities of these two lipids would promote GSL binding to Aβ. Another lipid, Cer, which is the hydrophilic backbone of GSLs, is known to be involved in exosome generation (23). We found higher levels of ceramide in exosomes than in cells (Fig. 7), consistent with a previous report (23).

Exosomes Are Incorporated into Microglia in Vitro and in Vivo, in a GSL-glycan-independent Manner—Our previous *in vitro* experiments demonstrated that engulfment of exosomes by mouse primary microglia occurred in a partially phosphatidylserine-dependent manner (8). However, deglycosylated proteins, *e.g.* immunoglobulin FC receptor, reportedly exhibit low affinity toward microglia (24). To determine whether cleavage of GSL-glycans would affect microglial uptake of exosomes, we exposed fluorescent-labeled exosomes pretreated with EGCase or PBS to microglial BV-2 cells. We found no decrease in microglial uptake of EGCase-treated exosomes (Fig. 8*A*). Both of the labeled exosomes were co-localized with the microglial marker Iba1 when intracerebrally injected into mouse brains (Fig. 8*B*), and there were no obvious differences observed between untreated or EGCase-treated exosomes. Few fluorescent exosomes were apparent in merged images of cells stained for either a neuronal or astroglial marker (Fig. 8*C*). The above data indicate that exosomes can be incorporated into microglia undisturbed by the absence of GSL-glycans on the membrane.

DISCUSSION

Our study presented here clearly demonstrated that intracerebral exosome infusion leads to a decrease in Aβ levels and ameliorates Aβ-related pathologies in APP mice. In the mouse brains, Aβ was trapped at the exosome surface by glycan moieties of GSLs and transported into microglia for degradation. Mass spectrometry-based analysis has revealed that GSLs are abundant in exosomes compared with parental cells. Just how GSLs are packed so much more into the exosomes than in parental cells remains an unanswered question. Exosomes are produced by intraluminal budding of the limited membrane of endosomes. Accumulation of Cer, which is generated by the hydrolysis of SM, has been reported to initiate the budding (23). Cer can induce a coalescence of small microdomains into larger